

# Monolithic Schottky-Collector Resonant Tunnel Diode Oscillator Arrays to 650 GHz

M. Reddy<sup>1</sup>, S.C. Martin<sup>2</sup>, A.C. Molnar<sup>1</sup>, R.E. Muller<sup>2</sup>, R.P. Smith<sup>2</sup>,  
P.H. Siegel<sup>2</sup>, M. J. Mondry<sup>1</sup>, M. J. W. Rodwell<sup>1</sup> and S.J. Allen, Jr.<sup>3</sup>

<sup>1</sup>Department of Electrical and Computer Engineering  
University of California, Santa Barbara, CA 93106

<sup>2</sup>California Institute of Technology  
Jet Propulsion Laboratory, Pasadena, CA 91109

<sup>3</sup>Center for Free-electron Laser Studies  
University of California, Santa Barbara, CA 93106

## **Abstract:**

We report the design, fabrication, and performance of monolithic, slot-antenna coupled Schottky-collector resonant tunnel diode (SRTD) oscillator arrays. A 64-element oscillator array oscillated at 650 GHz while a 16-element array produced 28  $\mu$ W at 290 GHz.

## **Introduction:**

Resonant tunnel diode (RTD) waveguide oscillators have been reported at frequencies as high as 712 GHz [1], well beyond the highest frequency transistor oscillators built to date [2]. Power levels achieved by discrete waveguide RTD oscillators are limited by constraints imposed on maximum device area for suppressing parasitic bias circuit oscillations [3]. Higher power levels can be obtained with monolithic RTD oscillators in which these constraints are eliminated by on-wafer bias stabilizers [4]. Power levels can then be further increased using quasi-optical array RTD oscillators [5]. Here, we report monolithic Schottky-collector RTD (SRTD) oscillator arrays with on-wafer Schottky-diode bias stabilizers. Different circuits operated at frequencies ranging from 100 GHz to 650 GHz. A 64-element array oscillated at 650 GHz. To our knowledge this is the highest oscillation frequency achieved by a monolithic oscillator. Additionally, a 16-element array produced 28  $\mu$ W at 290 GHz.

## **Design:**

The single element RTD oscillator circuit (Fig.1) consists of a 0.1  $\mu$ m InGaAs SRTD located in the center of a slot antenna terminated by air-bridged capacitors, resonant at the desired frequency of oscillation,  $f_{osc}$ . The SRTDs have a peak current density of  $5 \times 10^5$  A/cm<sup>2</sup> at a peak voltage of 0.95 V, a current peak to valley ratio of 1.7, a measured peak negative conductance of -19 mS/ $\mu$ m<sup>2</sup>, a parasitic capacitance of 3.0 fF/ $\mu$ m<sup>2</sup>, a parasitic resistance of 2.2  $\Omega$ - $\mu$ m<sup>2</sup> and a quantum well lifetime of 0.12 ps. These parameters are

normalized to the SRTD effective area which is twice the SRTD junction area to account for the spreading of electric field beneath the 0.1  $\mu\text{m}$  Schottky-collector. From the DC and microwave parameters, the 0.1  $\mu\text{m}$  InGaAs SRTD has an estimated maximum frequency of oscillation  $f_{\text{max}}$  of 2.2 THz [6], although such high  $f_{\text{max}}$  values are difficult to verify experimentally.

A low-impedance Schottky-diode and series resistor is located within  $\lambda_{\text{osc}}/4$  from the SRTD for suppressing both DC bistability and parasitic oscillations in the bias circuit at frequencies below the antenna's resonance [4]. The positive conductance of the low-impedance diode-resistor combination is larger than the absolute value of the SRTD's maximally negative conductance. The low-impedance diode's high turn-on voltage means that the diode-resistor combination can provide the low differential impedance while using only a small fraction of the current, and thus power consumption, that a resistor would use without the diode. The low-impedance Schottky diode is fabricated on AlInGaAs to give an appropriate amount of current and conductance in the negative-resistance voltage range of the RTD.

At the antenna's resonant frequency, the low-impedance Schottky-diode is decoupled from the SRTD and the SRTD is shunted only by the antenna's radiation impedance in series with the MIM capacitors. To ensure oscillation, the SRTD junction area is chosen such that the SRTD's negative conductance exceeds the antenna radiation conductance at  $f_{\text{osc}}$ . Interactions between neighboring slot antennas were ignored. In addition, the slot antennas were shortened in order to tune out the capacitances of the SRTDs.

More specifically, the approach used to design an oscillator of a given frequency is as follows: (1) Starting with a slot antenna with a resonant frequency somewhat higher than the design frequency, an appropriate SRTD with a sufficiently large negative conductance is chosen. (2) In order to move the oscillation frequency to the design value, the slot antenna size is altered to satisfy the relation:

$$\text{Im}[Y_{\text{ant}}] + \text{Im}[Y_{\text{srtld}}] = 0$$

at the design frequency, where  $\text{Im}[Y_{\text{ant}}]$  and  $\text{Im}[Y_{\text{srtld}}]$  are the imaginary parts of the admittances of the antenna and SRTD, respectively. SRTDs are chosen from the library of devices shown in table 1. Devices with stripe lengths  $> 4 \mu\text{m}$  had been observed to fail due to overheating, so devices with stripe lengths of 6 and 8  $\mu\text{m}$  consisted of two 3  $\mu\text{m}$  or 4  $\mu\text{m}$  stripe length SRTDs connected in parallel.

Larger SRTD junction areas provide design margin but also detune the slot antenna from its resonant frequency due to an increased parasitic SRTD capacitance. The maximum SRTD junction area per single element oscillator was  $0.8 \mu\text{m}^2$  to prevent device burnout at the high operating current density. SRTD oscillator arrays were designed with varying slot antenna lengths and varying SRTD junction areas with the objective of building oscillators in the 100 GHz to 1000 GHz frequency range. The arrays were obtained by

repeating the single element slot antenna coupled oscillator (Fig. 1) into rows and columns. The separation between the adjacent elements for various frequency array designs was chosen to be less than the corresponding half wavelength in the substrate to ensure a single main lobe in the radiation pattern of the antenna arrays.

Array fabrication requires monolithic integration of 0.1  $\mu\text{m}$  InGaAs SRTDs, Schottky-diode bias stabilizers, MIM capacitors, N<sup>++</sup> resistors, slot antennas and airbridges. The molecular beam epitaxial layer structure (Fig. 2) consists of graded bandgap AlInGaAs Schottky-diode [7] layers grown beneath the InGaAs SRTD layers. The SRTD layers consist of 5 monolayer AlAs barriers in the double barrier heterostructure which yield current densities in the vicinity of  $5 \times 10^5 \text{ A/cm}^2$ . Fabrication (Fig. 3) starts with exposing the Schottky-diode surface layers by etching away the SRTD layers in regions where the bias stabilizer is required. A non-selective etch (3:1:50,  $\text{H}_3\text{PO}_4 : \text{H}_2\text{O}_2 : \text{H}_2\text{O}$ ) is used to etch away most of the layers and stop within the 1000  $\text{\AA}$  AlInAs layer. A selective etch (1:1:4:1,  $\text{CH}_3\text{COOH} : \text{HBr} : \text{HCl} : \text{H}_2\text{O}$ ) then removes the remaining AlInAs layer and stops on the InGaAs cap layer of the Schottky-diode. Subsequently, ohmic contacts to the N<sup>++</sup> layers of both the SRTD and the Schottky-diode are formed by first recess etching and then depositing and annealing Au-Ge-Ni metal. The 0.1  $\mu\text{m}$  Schottky-collector for the SRTD is then defined using an airbridge electron beam collector process [8] (Fig. 4). Mesa isolation is achieved using a wet etch (3:1:50,  $\text{H}_3\text{PO}_4 : \text{H}_2\text{O}_2 : \text{H}_2\text{O}$ ) and is followed by interconnect metal deposition (Ti/Pt/Au). A 1000  $\text{\AA}$  thick, PECVD SiN film is then patterned to access both the bottom plate of the MIM capacitors and the surface layers of the Schottky-diode. Posts and evaporated airbridges provide the second level of interconnections, the top plate of the MIM capacitors and the stabilizer diode's Schottky-contact metal. A layout of an array is shown in Figure 5.

### **Results:**

The arrays were tested with a quasi-optical configuration (Fig. 6). The 23 mm diameter Si hyperhemispherical lens on which the oscillator array is placed forms the array's external resonant cavity, determining both the oscillation frequency and the oscillator Q. For arrays oscillating below 250 GHz, the oscillator array output was detected directly using a broad band bowtie-antenna-coupled Schottky diode harmonic mixer. The harmonic mixer downconverts the signal frequency to the 2-12 GHz passband of a spectrum analyzer. A 2-element array oscillated at 109 GHz (Fig. 7(a)). A second 2-element array having shorter slot length oscillated at 196 GHz (Fig. 8). A 16-element array oscillated at 94 GHz [9](Fig. 7(b)). This array radiated 5% of its output power into a secondary cavity mode at 108 GHz.

For arrays oscillating above 250 GHz, the signals were detected by a liquid helium cooled Ge bolometer or a less sensitive but calibrated Thomas acousto-optic bolometer. A Fabry-Perot interferometer measures the signal wavelength and hence the frequency. A 64-element array produced oscillations at 650 GHz (Fig. 9). Other arrays oscillated at 290 GHz, 300 GHz, 310 GHz, 470 GHz and 560 GHz (Table 2).

The output power of a 16-element array oscillating at 290 GHz was measured to be  $28 \pm 2 \mu\text{W}$  by the acousto-optic power detector. This corresponds to a  $440 \text{ W/cm}^2$  power per unit SRTD junction area. This measured power does not correct for reflection and diffraction losses in the beam path, which may be substantial. Power measurements of the higher frequency oscillator arrays using the acousto-optic detector proved difficult as the power levels were close to the instrument's threshold and a Ge bolometer was then used instead. Direct electrical connection to the individual SRTDs is not possible at submm-wave frequencies. Therefore, we cannot conclusively establish that every array element is oscillating. However, we note that except for the 100 GHz designs (where both the 2-element and the 16-element arrays have similar total SRTD junction areas) the detected signal levels of the 16-element oscillator arrays are approximately an order of magnitude larger than the 2-element oscillator arrays.

For designs above 500 GHz, the slot length becomes comparable to the capacitor, stabilizer diode and the SRTD dimensions. The physical layout then fails to conform well to a slot antenna. We believe that the highest oscillation frequency (650 GHz) obtained is limited by these layout considerations. More recent work [10] indicates that much more compact SRTD layouts could be fabricated, and the use of structure simulators could be used to correct for any such effects in future designs.

#### **Acknowledgements:**

The UCSB work is supported by ONR under contract N00014-93-0378, NSF (QUEST) and AFOSR. The JPL work was performed at the JPL Center for Space Microelectronics Technology, and was sponsored by the NASA Office of Space Science. The authors wish to acknowledge discussions with H.S. Tsai and R.A. York from the University of California, Santa Barbara.

Design	A ( $\mu\text{m}^2$ )	Length ( $\mu\text{m}$ )	$G_n$ (mS)	$C_{rtd}$ (fF)	$L_{qw}$ (pH)	$R_s$ ( $\Omega$ )
SR2	0.4	2.0	7.6	1.2	15.8	5.5
SR3	0.6	3.0	11.4	1.8	10.5	3.66
SR4	0.8	4.0	15.2	2.4	7.9	2.76
SR5	1.2	6.0	22.8	3.6	5.26	1.94
SR6	1.6	8.0	30.4	4.8	3.96	1.38

Table 1: Small-signal model parameters for the various 0.1  $\mu\text{m}$  SRTDs in the device library. In this table, A represents the effective area as inferred from capacitance extraction, which is twice the SRTD junction area.

# of array elements	Total SRTD area ( $\mu\text{m}^2$ )	Slot length ( $\mu\text{m}$ )	Osc. freq (GHz)
16	3.2	544	94
2	1.6	430	109
2	1.6	217	196
16	6.4	157	290
16	12.8	121	300
2	1.6	121	310
16	6.4	84	470
16	6.4	53	560
64	19.2	51	650

Table 2: Summary of results obtained with various SRTD oscillator arrays designed with parameter variation of total SRTD junction area, slot antenna length and number of unit cell elements in the array.

**References:**

- [1] E.R. Brown, J.R. Soderstorm, C.D. Parker, L.J. Mahoney, K.M. Molvar and T.C. McGill, "Oscillations up to 712 GHz in InAs/AlSb resonant-tunneling diodes," *Appl. Phys. Lett.*, vol. 58, no. 20, pp 2291-2293, May, 1991.
- [2] S.E. Rosenbaum, B.K. Kormanyos, L.M. Jelloin, M. Matloubian, A.S. Brown, L.E. Larson, L.D. Nguyen, M.A. Thompson, L.P.B. Katehi and G.M. Rebeiz, " 155 and 213-GHz AlInAs/GaInAs/InP HEMT MMIC Oscillators", *IEEE Transactions on Microwave Theory and Techniques*, vol. 43, no. 4, pp. 927-932, April, 1995.
- [3] C. Kidner, I. Mehdi, J.R. East and G.I. Haddad, "Bias circuit instabilities and their effect on dc current-voltage characteristics of double-barrier resonant tunneling diodes," *Solid-State Electron.*, vol. 34, no. 2, pp 149-156, Feb., 1991.
- [4] M. Reddy, R.Y. Yu, H. Kroemer, M.J.W. Rodwell, S.C. Martin, R.E. Muller and R.P. Smith, "Bias stabilization for resonant tunnel diode oscillators," *IEEE Microwave and Guided Wave Lett.*, vol. 5, no. 7, pp. 219-221, July, 1995.
- [5] M.P. De Lisio, J.F. Davis, S.J. Li, D.B. Rutledge and J.J. Rosenberg, "A 16-element tunnel diode grid oscillator," *IEEE AP-S International Symposium*, Newport Beach, CA, June, 1995.
- [6] M. Reddy, M.J. Mondry, M.J.W. Rodwell, S.C. Martin, R.E. Muller, R.P. Smith, D.H. Chow and J.N. Schulman "Fabrication and dc, microwave characteristics of submicron Schottky-collector AlAs/In<sub>0.53</sub>Ga<sub>0.47</sub>As/InP resonant tunneling diodes," *J. Appl. Phys.*, vol. 77, no. 9, pp. 4819-4821, May, 1995.
- [7] D.H. Lee, S.S. Li, N.J. Sauer, and T.Y. Chang, "High quality In<sub>0.53</sub>Ga<sub>0.47</sub>As Schottky diode formed by graded superlattice of In<sub>0.53</sub>Ga<sub>0.47</sub>As/In<sub>0.52</sub>Al<sub>0.48</sub>As," *Appl. Phys. Lett.* , vol. 54, no. 19, pp. 1863-1865, May, 1989.
- [8] R.E. Muller, S.C. Martin, R.P. Smith, S.T. Allen, M. Reddy, U. Bhattacharya and M.J.W. Rodwell. "Electron-beam lithography for the fabrication of air-bridged, submicron Schottky-collectors," *J. Vac. Sci. Technology B*, vol. 12, no. 6, pp. 3668-3672, Nov Dec, 1994.
- [9] M. Reddy, M.J. Mondry, A.C. Molnar, U. Bhattacharya, M.J.W. Rodwell, S.C. Martin, R.E. Muller and R.P. Smith. "Monolithic RTD array oscillators at 100 GHz and 200 GHz with on-wafer bias stabilization." *Late news, 54th Annual Device Research Conference*. Santa Barbara, CA, June, 1996.
- [10] R.P. Smith, S.C. Martin, M. Kim, J. Bruston, D. Humphrey, N. Erickson, and P.H. Siegel. "Advances in Submillimeter Wave Semiconductor-Based Designs and Processes at JPL." to be published in the *Proceedings of the 8<sup>th</sup> Space Terahertz Symposium*, Cambridge, MA, March, 1997.

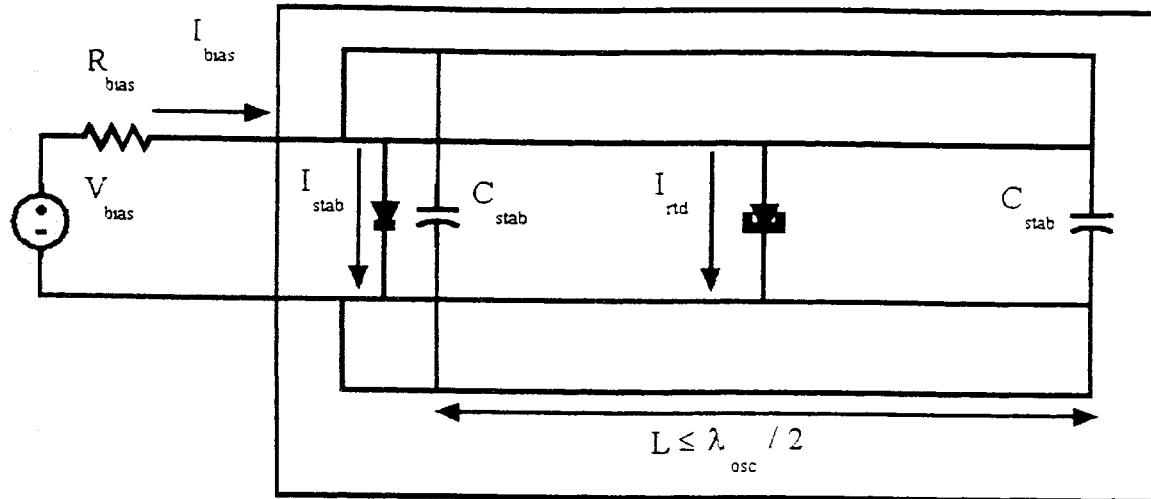


Figure 1: Circuit schematic of a monolithic slot-antenna coupled SRTD oscillator.

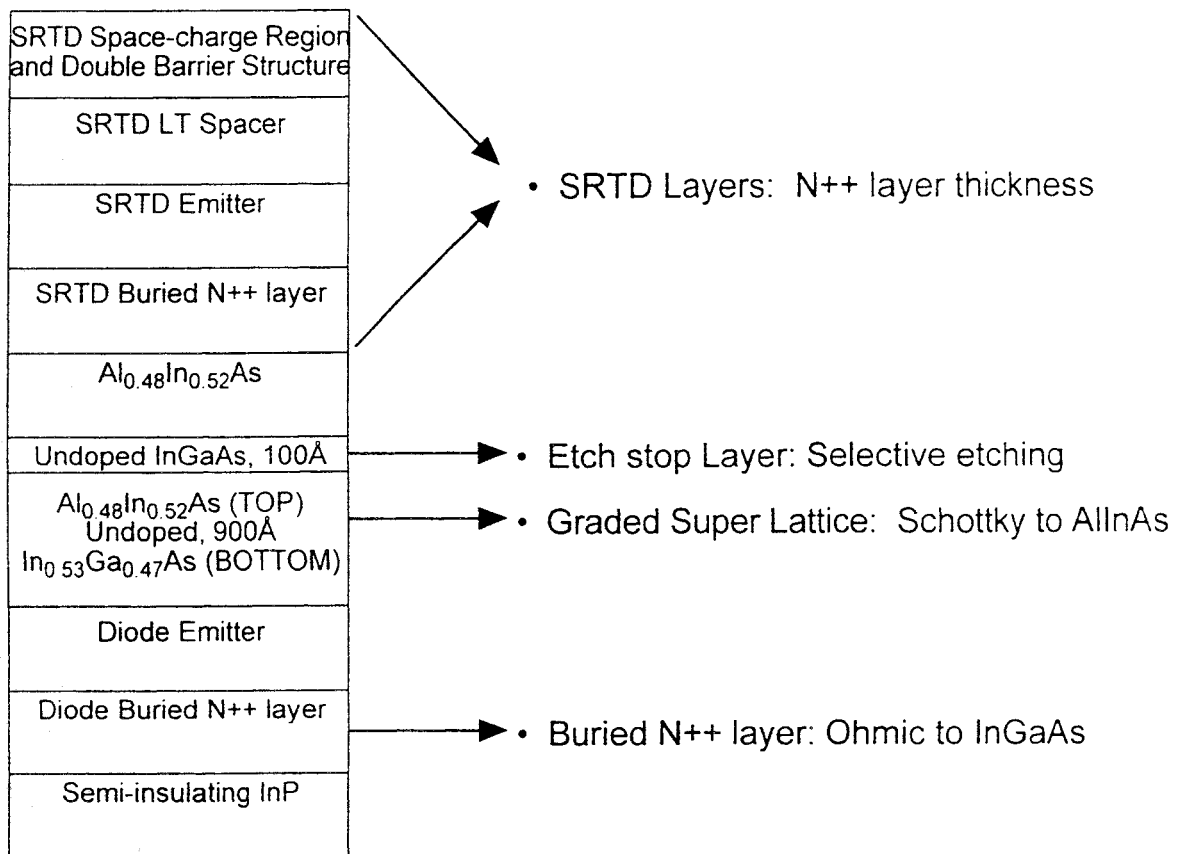


Figure 2: Layer structure grown by molecular beam epitaxy (MBE) for SRTDs, bias stabilization diodes, and resistors on semi-insulating  $InP$  substrates.

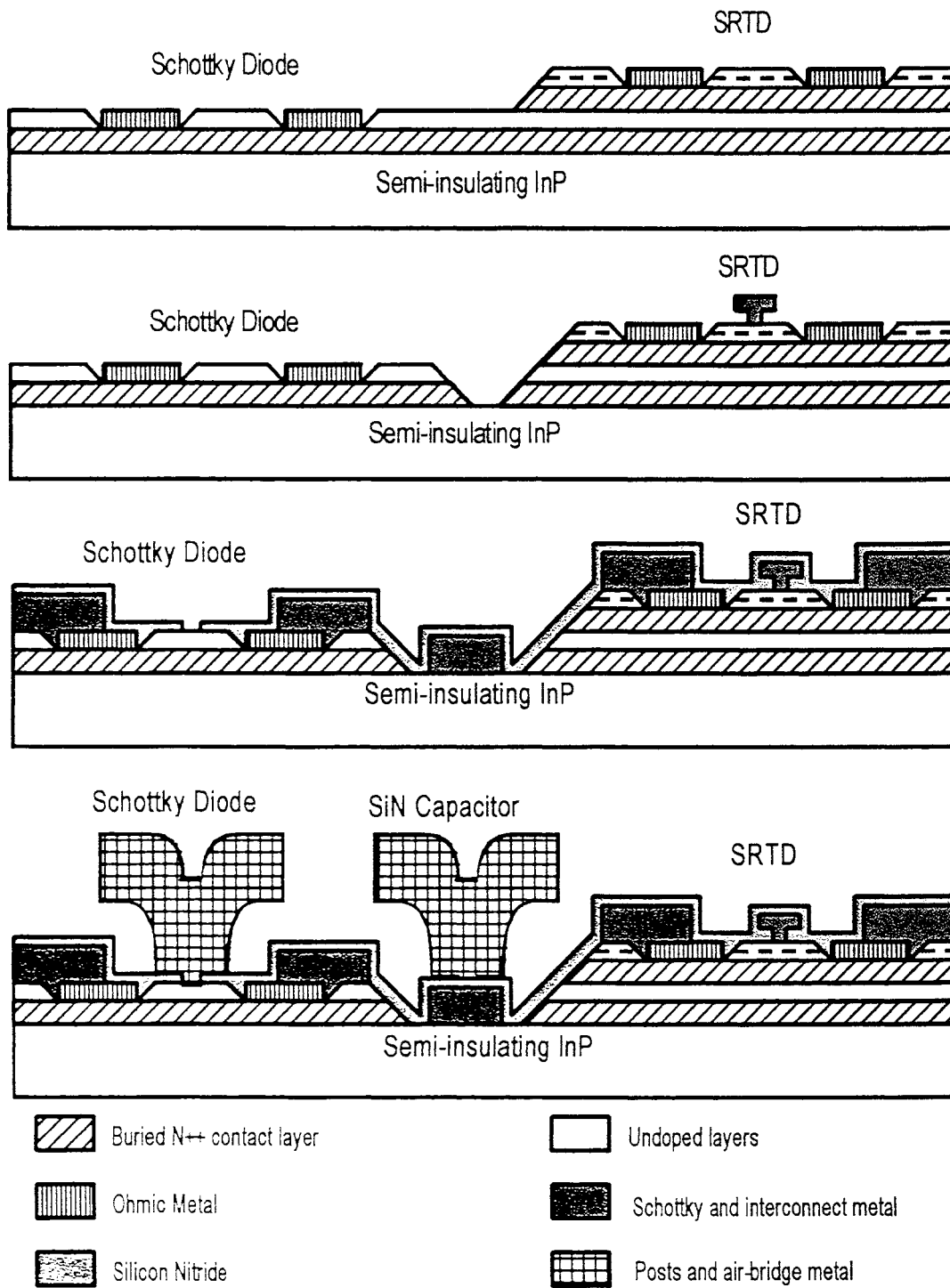


Figure 3: The process steps are: a) etching down to the stabilizer region, then depositing and annealing the ohmic contacts, b) defining the Schottky collectors and etching the mesas, and c) depositing interconnect metal, and then depositing and patterning silicon nitride for passivation and capacitor dielectrics, and d) fabricating the air-bridges and capacitor top plates.



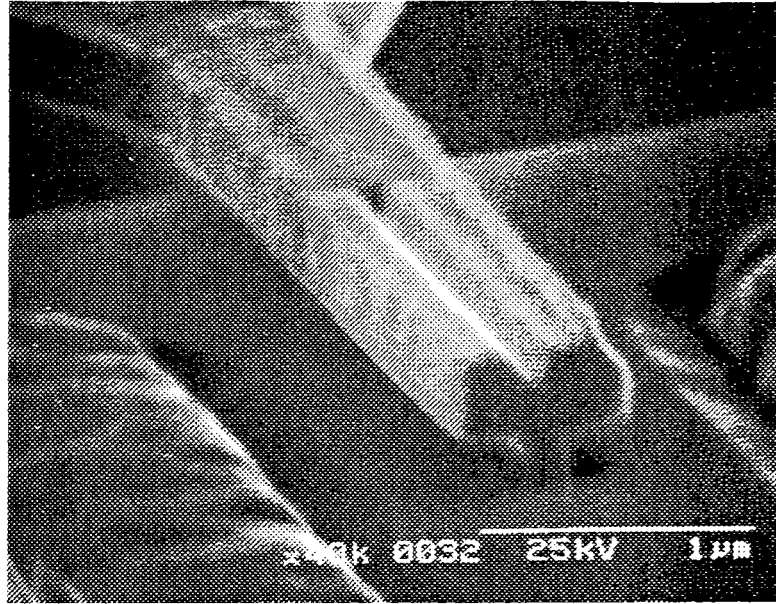


Figure 4: SEM photograph of a 0.1  $\mu\text{m}$  InGa.As SRTD

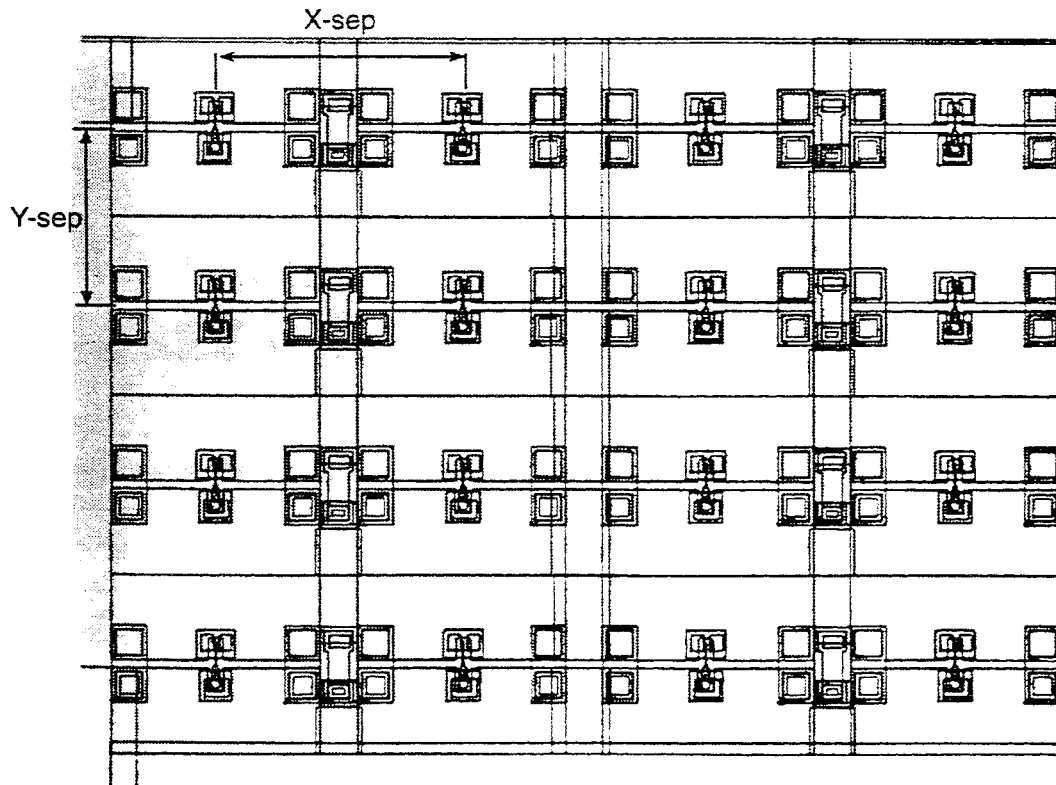


Figure 5: Mask layout of a 16-element array oscillator. The layout for array designs is obtained by simply repeating the single-element layout in the X and Y directions.

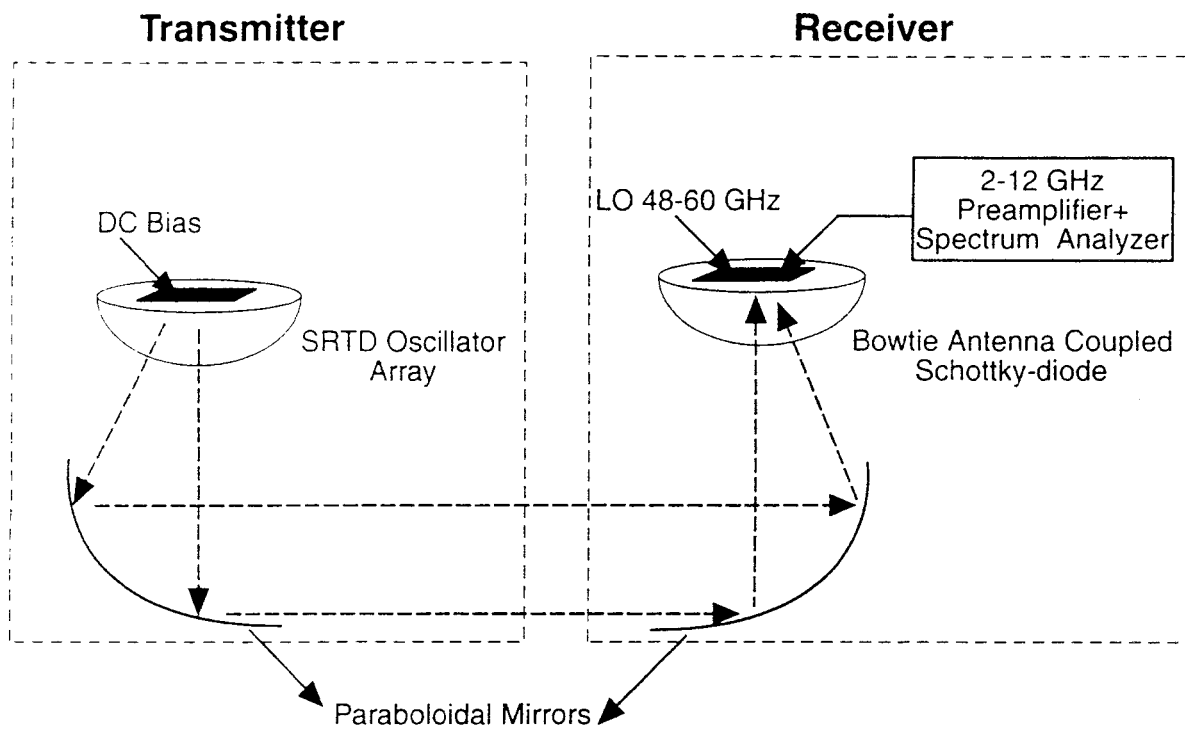
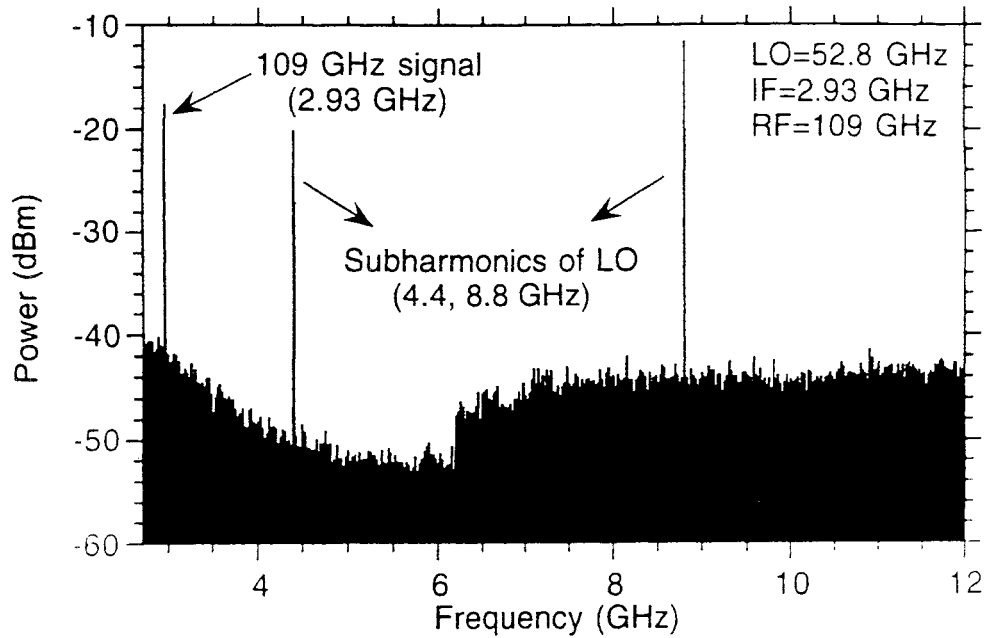
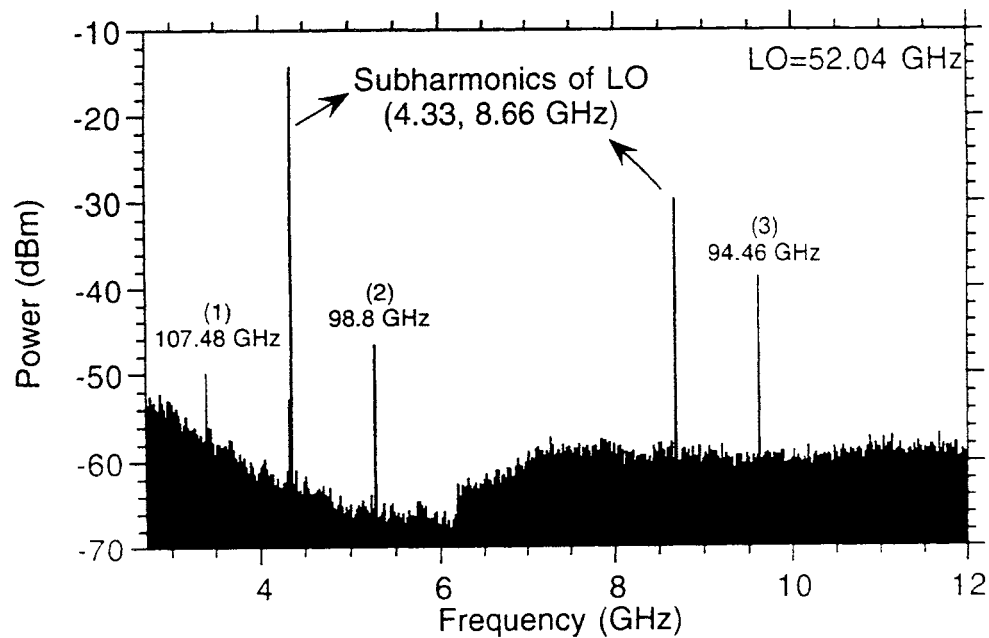


Figure 6: Quasi-optical oscillator array on a silicon lens which forms the oscillator's resonant cavity.



a.



b.

Figure 7: Measurements of oscillator arrays: Spectra of (a) 2-element and (b) 16-element arrays at near 100 GHz showing multiple oscillation frequencies for the 16-element array. In both cases the linewidth is limited by the measurement system.

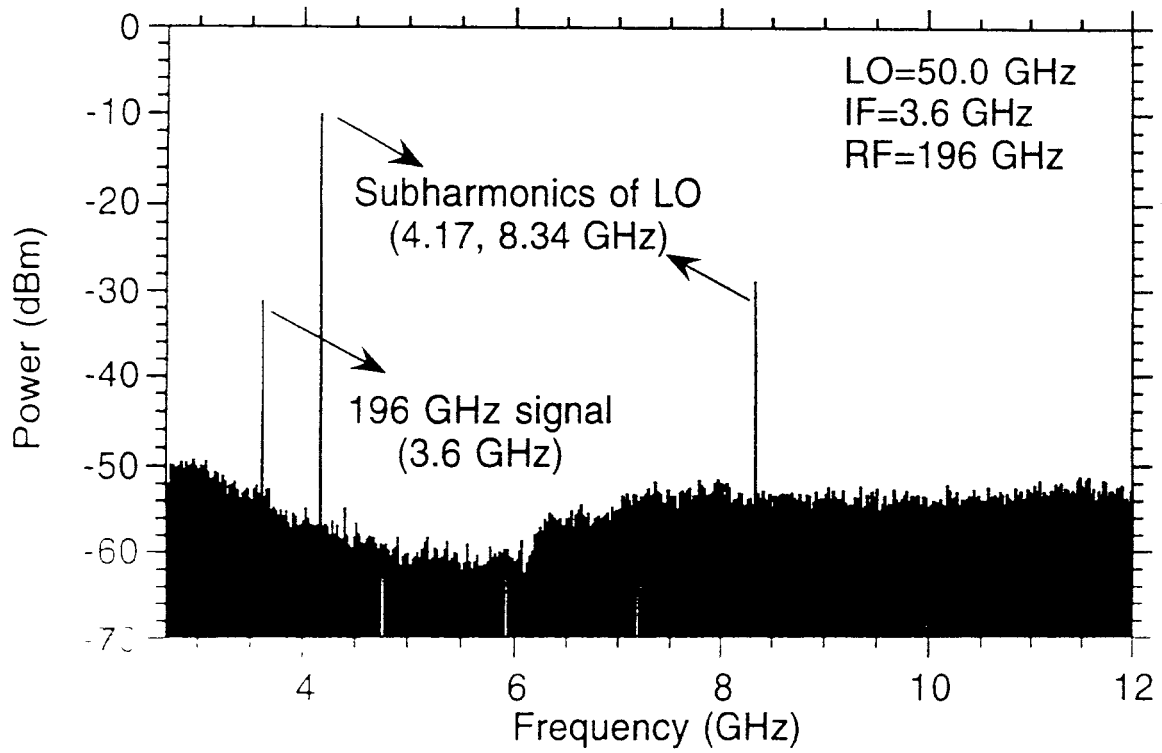
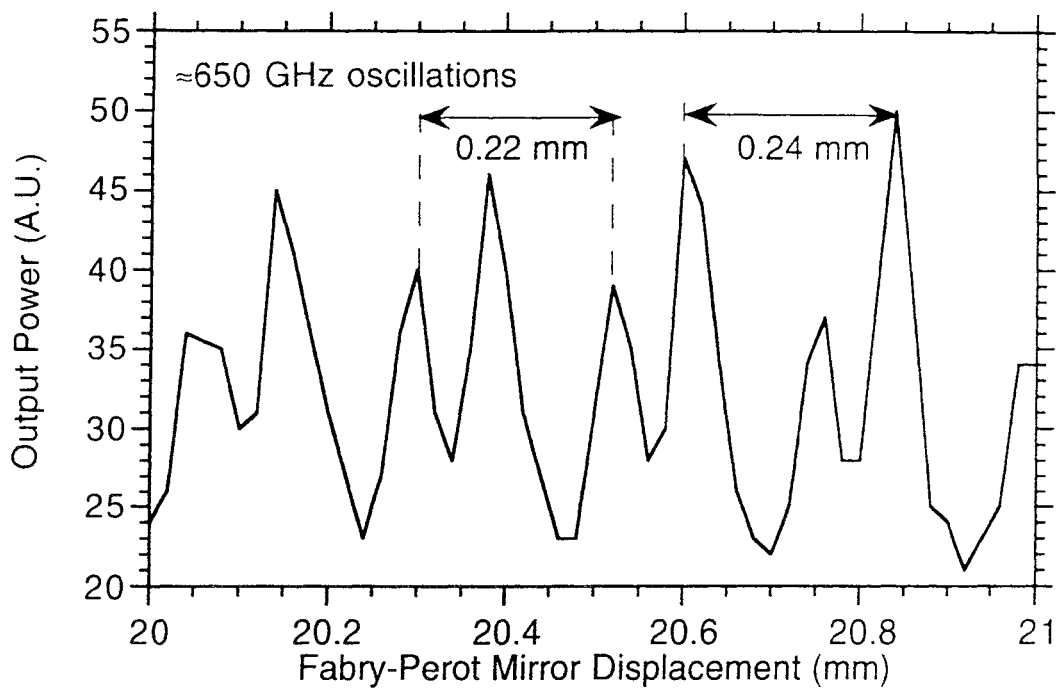
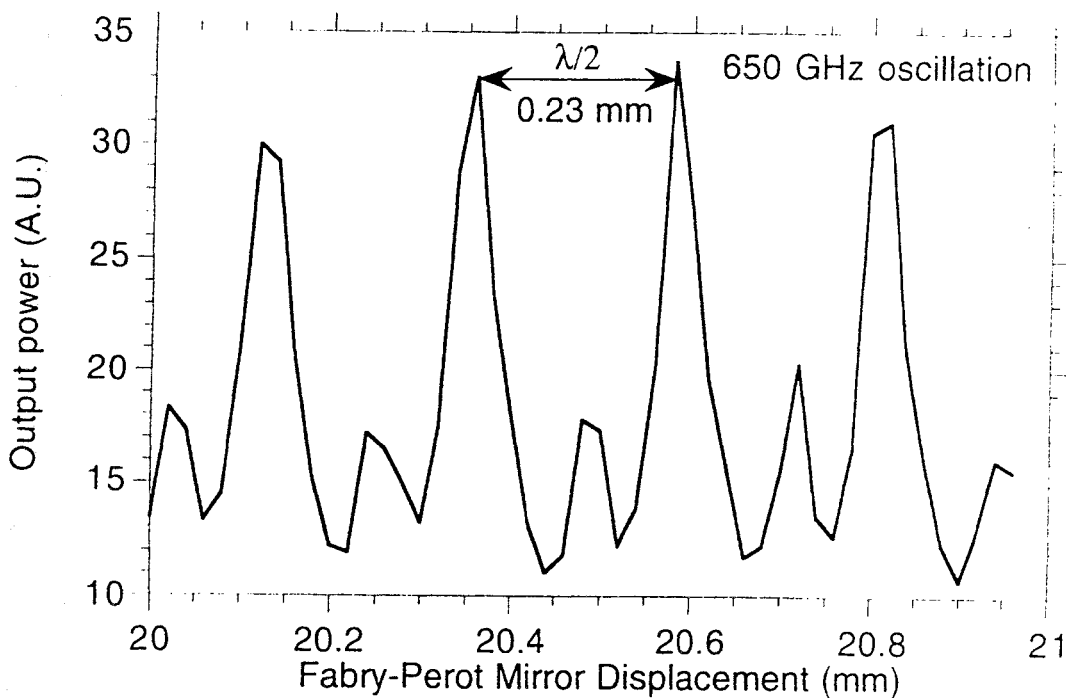


Figure 8: Spectrum of a 2-element array at 196 GHz tested with a Schottky-diode harmonic mixer.



a.



b.

Figure 9: Detected power of a 64-element array as a function of Fabry-Perot interferometer cavity length showing transmission peaks separated by 0.23 mm (a 650 GHz signal). In (b) the substrate was separated from the silicon lens by a 0.8 mm air gap.